Catalysis Letters 39 (1996) 219–231

An HREM study of the WO_3/TiO_2 monolayer catalyst system. Proposals for the overlayer structure

Andy Burrows [a,1], Christopher J. Kiely [a], Richard W. Joyner [b], Helmut K. Knözinger [c] and Friederike Lange [d]

[a] *Department of Materials Science and Engineering, The University of Liverpool, PO Box 147, Liverpool L69 3BX, UK*
[b] *Catalysis Research Centre, Nottingham Trent University, Clifton Lane, Nottingham NG11 7NS, UK*
[c] *Institut für Physikalische Chemie, Universität München, Sophienstrasse 11, D-80333, Munich, Germany*
[d] *Abteilung Anorganische Chemie, Fritz-Haber-Institut der Max-Planck-Gesellschaft,*
Faradayweg 4-6, 14195 Berlin, Germany

Received 22 February 1996; accepted 12 March 1996

High resolution electron microscopy (HREM) has been used to characterise the WO_3/TiO_2 (anatase) catalyst system. Comparisons between pure samples of TiO_2 in the uncalcined and calcined states with titania in the catalyst (loaded with 10 wt% WO_3) indicate that the tungsten oxide overlayer preserves the surface roughness of the support (as observed in the pure uncalcined material). The calcination of pure anatase results in significant grain growth and surface smoothing. In the electron microscope, the tungsten oxide overlayer is revealed as 2D pseudo-hexagonal shaped clusters which appear to be epitaxially related to the support. After noting that the anatase support predominantly exposes {112}, {011}, {110} and (001) type facets we have combined this information with structural data on the overlayer derived from a previous EXAFS and XANES study by Hilbrig et al. that reported the presence of WO_4 species and six-coordinate WO_5 groups. By considering the arrangement of terminating oxygen atoms on each of the aforementioned anatase surfaces, we suggest ways in which the WO_x species may be linked together to form the tungsten oxide overlayer. This approach has led us to conclude that, with the exception of the (001) surface, the overlayer may consist of WO_4 dimers rather than chains of linked WO_5 groups terminated by WO_4 species.

Keywords: high resolution electron microscopy; tungsten oxide; titania; WO_3/TiO_2 catalyst system; structural models

1. Introduction

Emissions of nitrogen oxides (NO_x) into the atmosphere from carbonaceous fuel burning sources are well known to cause environmental damage. For the case of pollution caused by the motor car, this problem has been addressed successfully by the use of the three-way automotive catalyst [1]. More recently, stationary sources, such as power stations, have increasingly become the subject of stringent legislation and hence there is a growing interest in the structure and function of catalysts used for stack-gas cleaning.

The most widely adopted method of stack-gas cleaning involves selective catalytic reduction (SCR) of the emissions by adding ammonia in controlled amounts to promote the following reaction:

$$6NO + 4NH_3 \rightarrow 5N_2 + 6H_2O$$

Although typical NO_x concentrations discharged are low, they are usually accompanied by excess oxygen and in terms of the suitability of a catalyst, oxidation to NO_2 must be avoided. The most effective materials that meet this criterion have been found to be the so-called *monolayer* catalysts typically derived from the oxides of vanadium, molybdenum and tungsten supported on a suitable substrate, e.g. TiO_2 [2]. Despite the wealth of knowledge that has accumulated in recent times concerning the chemical nature (structural units, bond lengths, oxidation states etc.) of this type of catalyst [3,4], there are few studies reported which attempt to combine this data with details of the *support* structure to arrive at an overall structural model for the overlayer.

In this paper, we present a TEM study of the WO_3/TiO_2 (anatase) catalyst with a view to identifying plausible structural models for the tungsten oxide overlayer. Particular reference is made to previous investigations of this system by Hilbrig et al. [5,6], who used XANES and EXAFS and CO adsorption measurements in identifying individual WO_x structural units. They also proposed a very tentative model for the overlayer based on linked chains of WO_5 groups terminated by WO_4 species. We will show that the crystallographic habit of the TiO_2 support consistently exposes certain types of facet plane and this information can be used to deduce the most likely anchor sites of the previously identified WO_x units.

2. Experimental

The tungsten oxide on titania (pure anatase) catalysts were prepared by aqueous impregnation of the TiO_2 from an ammonium metatungstate solution (pH = 4) to give a loading of 10 wt% WO_3. The resulting paste was

---

[1] To whom correspondence should be addressed.

then dried at 110°C overnight and subsequently calcined in wet air at 620°C for 7 h. The loading was purposely chosen to avoid exceeding the monolayer capacity of the support, the intention being to aid the TEM observations. For comparison purposes, two samples of pure anatase TiO_2 were also studied: one in the uncalcined state and the other calcined under the same conditions as the WO_3/TiO_2 catalyst. TEM samples were prepared by gently grinding the powdered materials in the presence of ethanol and a single drop of the resulting slurry deposited on a carbon coated copper grid. The sample was then examined in a Jeol 2000EX high resolution electron microscope. Since both the anatase form of TiO_2 and WO_3 can be reduced by the action of the electron beam [7,8], the micrographs presented were all recorded within a few seconds of locating an area of interest. Occasionally, as a means of verifying the structural validity of the photographically recorded micrographs, images were obtained under low illumination conditions by utilising a low light level TV camera and frame averaging system (thus minimising radiation damage effects). High resolution image simulations were performed using the EMS software package [9].

3. Results

Figs. 1a and 1b are axial HREM [111] images of the pure uncalcined and calcined TiO_2 respectively. The uncalcined material has a grain size distribution of 20–30 nm and typically has rough surfaces consisting of many microfacets of the order of 5–35 Å in length ({112} and {011} facet types are evident in this micrograph). Albeit rarely, longer facets have also been observed on some grains that extend up to 170 Å. By contrast, pure calcined anatase grains are much more regular and consistently exhibit facet lengths in the region of 120–210 Å. The grain size distribution (30–50 nm) is also significantly larger and the exposed surfaces are smoother due to the calcination treatment. The facets exposed by the particular grain in fig. 1b are {101}, {011} and {112} type.

An image from a support grain in the WO_3/TiO_2 catalyst is shown in fig. 1c. The particle is oriented on the [021] zone axis of TiO_2 and shows strong {112} facetting. It is apparent that the presence of WO_3 preserves the surface roughness of the support as noted for the pure uncalcined TiO_2, i.e. the anatase surfaces are also microfacetted with similar microfacet lengths of between 5 and 35 Å. The overall grain size distribution (30–50 nm) is comparable to that observed in calcined TiO_2.

BET surface area measurements were carried out for the two pure TiO_2 samples and the chemically prepared WO_3/TiO_2 catalyst. Uncalcined TiO_2 was found to have a large surface area of 97 $m^2\ g^{-1}$ consistent with the observation that it comprises relatively small highly facetted particles. A reduction in surface area to 55 $m^2\ g^{-1}$ for the pure calcined sample is compatible with the observed surface smoothing and grain growth resulting in the increased length of exposed facets. Samples of the WO_3/TiO_2 catalyst have surface areas (72 $m^2\ g^{-1}$) intermediate between that of the uncalcined and calcined pure TiO_2 materials. This loss of surface area compared to uncalcined TiO_2 is simply attributable to the grain growth occurring during calcination. On the other hand, the higher value of surface area, but comparable overall grain size (30–50 nm) as compared to pure calcined TiO_2, is due to the preservation of a greater number and shorter size range of surface facets. It was also apparent that particular low index zone axes could frequently be resolved which has led us to conclude that the predominant surface planes exposed by anatase in order of observed frequency are {112}, {011}, {110} and (001) types.

A distinguishing feature of the titania support grains in the "monolayer" catalyst material is the occurrence of dark specks on individual support particles (arrowed in fig. 1c) which are absent on either of the two pure samples of anatase. Since EDX analysis reveals the presence of tungsten oxide on the catalyst support, we believe the specks, which are in general hexagonal shaped, are due to contrast from the tungsten oxide overlayer.

3.1. The tungsten oxide overlayer – theoretical models

Studies of other transition metal oxide supported catalysts indicate that the structure of an overlayer is dependent on the extent of surface coverage [4,5]. For less than monolayer coverage, the conclusion seems to be that an overlayer will consist of polymeric MO_x type chains and perhaps monomeric MO_x units. At and beyond the monolayer capacity of the support, discrete crystallites of the supported oxides are formed such as the tower structures proposed by Bond et al. [10] for MoO_3/TiO_2 and WO_3/TiO_2 catalysts. This particular aspect is not an issue in this study since the WO_3 loading was deliberately chosen *not* to exceed the monolayer capacity of the anatase support, and in any case, no 3D tungsten oxide crystallites were ever seen in profile.

In a detailed structural study by Hilbrig et al. [5] on WO_3/TiO_2 using EXAFS and XANES, separate tetrahedral WO_4 species and pentahedral WO_5 units attached to the titania surface via W–O–Ti bonds were identified (the two types of polyhedra are shown in fig. 2a). The WO_4 groups were found to predominate at loadings of approximately 1/3 of a monolayer and less whilst WO_5 units were more abundant at loadings approaching the monolayer capacity of the support. Their postulated structure for the overlayer (which is not isostructural with the known forms of WO_3) then consisted of branched WO_5 chains (W–O–W bridged) terminated by

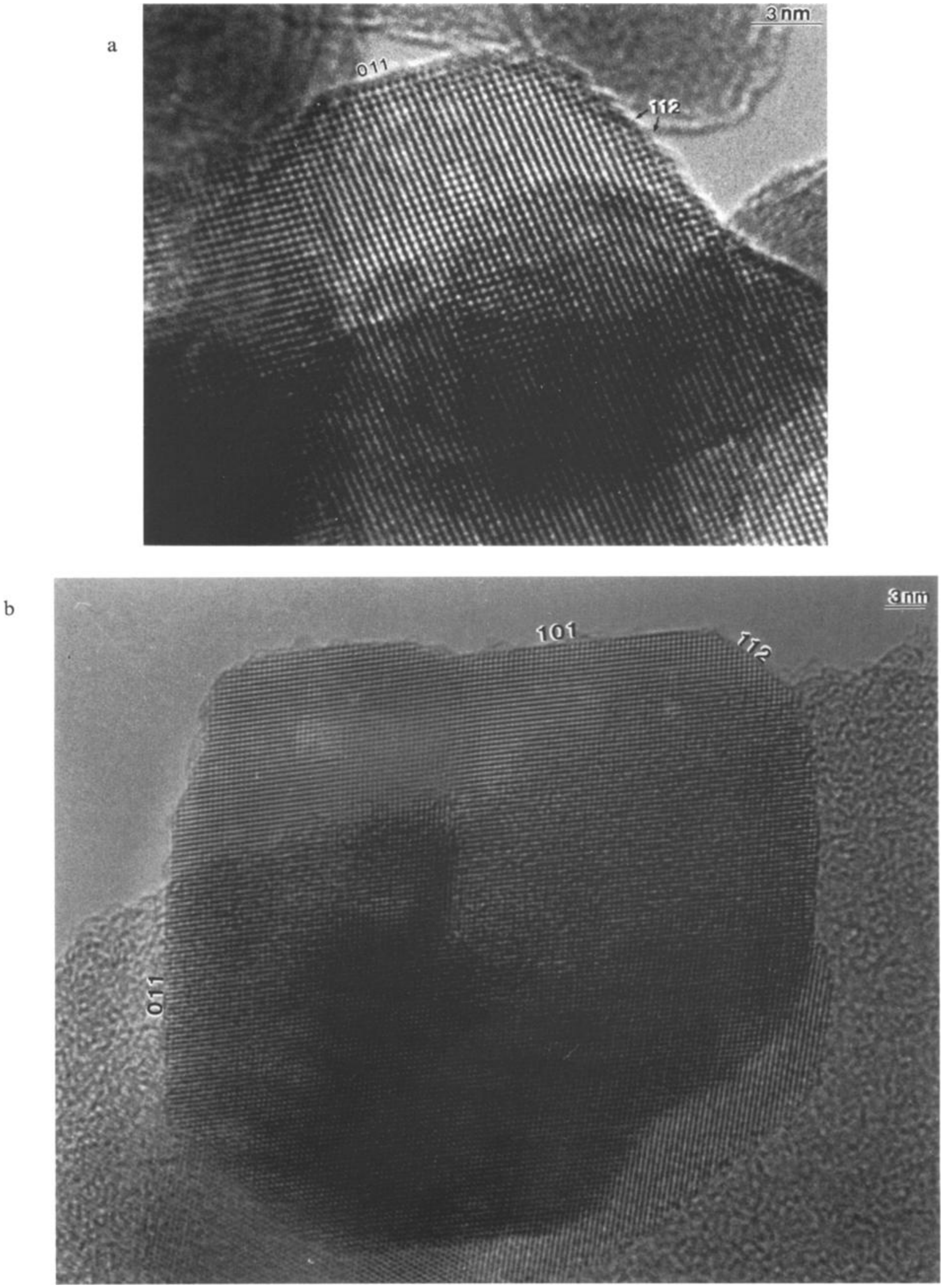

Fig. 1. (a) An axial [111] HREM image of a TiO_2 grain observed in the uncalcined pure material showing {011} and {112} facets. (b) An axial [111] HREM image of a TiO_2 grain observed in the calcined pure material showing {011}, {101} and {112} facets. (c) A particle of titania (oriented on the [021] anatase zone axis) observed in the WO_3/TiO_2 sample showing strong {112} facetting. Pseudo-hexagonal clusters apparently epitaxially related to the support are arrowed.

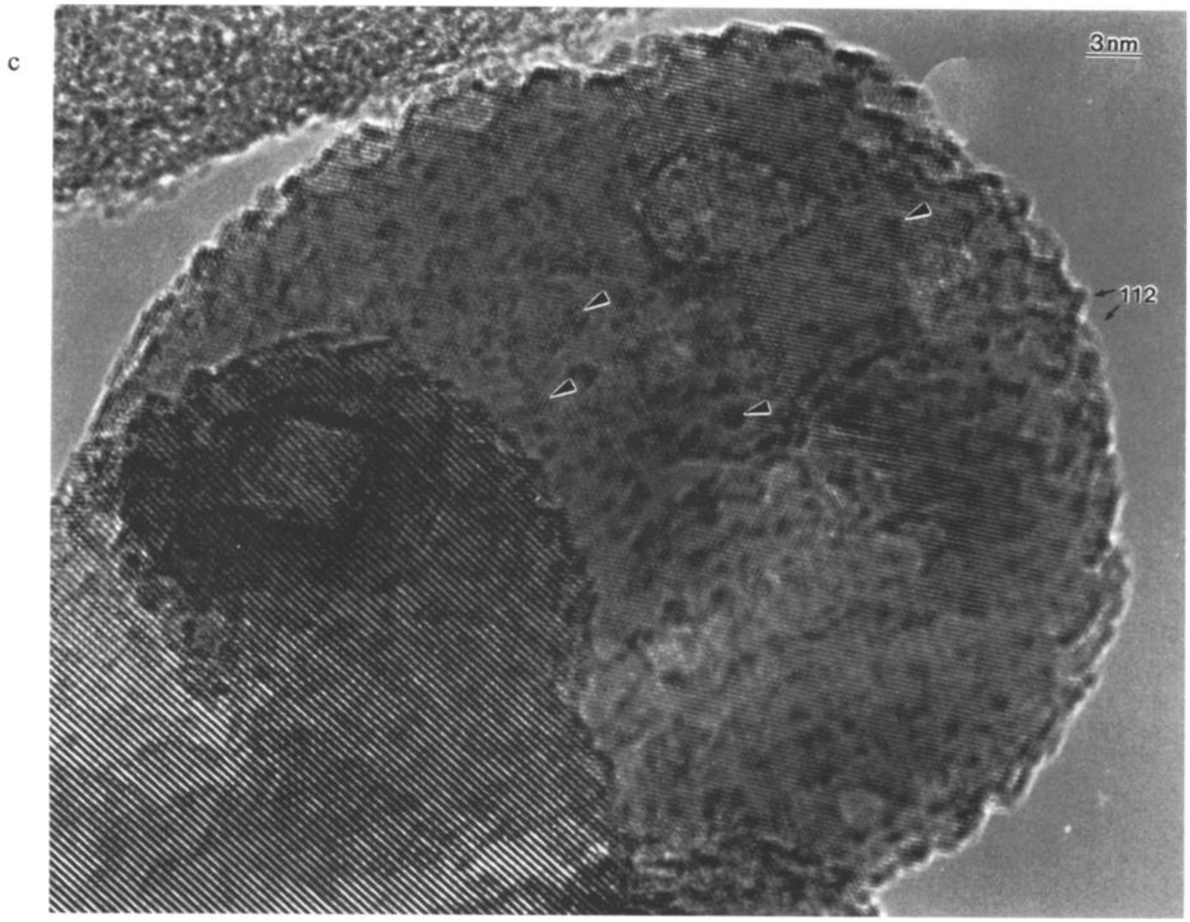

Fig. 1. (Continued.)

the WO_4 groups. A schematic representation of the Hilbrig et al. model is shown in fig. 2b, although no particular terminating surface was specified for the titania support. Two W–O distances were reported: (i) 1.76 Å, attributed to the W=O bond and (ii) 1.91 Å, attributed to the W–O bond in the W–O–W and W–O–Ti bridges respectively. A characteristic distance of 2.92 Å was also derived from the EXAFS spectrum which was very tentatively related to a W–O–Ti anchoring bond. Given the electron microscopy results of this study have demonstrated that the predominantly exposed anatase support surfaces are {112}, {011}, {110} and (001) types, it is logical to try and fit the WO_x structural units (using the appropriate bond length data) to the arrangement of terminating oxygen atoms displayed by each of these surfaces. Whilst it is recognised that the titania surfaces are likely to be reconstructed, or at least relaxed under the influence of the tungsten oxide overlayer, there is no information available on the nature of these changes for the planes of interest here. The best assumption we can make, therefore, is that the anatase planes exhibit their bulk termination structure.

The arrangement of straight chains and the branching that was postulated by Hilbrig et al. would place a possible branching oxygen perpendicular to the chain with a 30° inclination of the W–O bond to the substrate plane (assuming ideal trigonal bipyramidal symmetry). However, there is another plausible way to connect WO_5 units (fig. 2c) where the W–O–W bonds lie in a plane parallel to the substrate surface with all of the oxygen double bonds perpendicular to this plane. The spine of the chain now has a zig-zag pattern of WO_5 units at an angle of 120° to each other. An arrangement such as this could also lead to (in principle at least) closed ring structures (fig. 2d).

Various views of the (001), (011), (112), and (110) oxygen terminated planes are shown in figs. 3–6 respectively. For each of them a view normal to the surface is shown in (i) revealing the projected arrangement of oxygen and titanium atoms. A profile view of the unrelaxed surface is shown in (ii) whilst the figure labelled (iii) shows only those oxygen atoms that are close to a terminating facet plane and how, in principle, linked WO_5 and WO_4 structural units are most likely to be arranged on the support surface. If it is presumed that the individual WO_5 and WO_4 units assume ideal trigonal bipyramidal and tetrahedral symmetry respectively, it is apparent that anchoring polymeric tungsten oxide chains to the

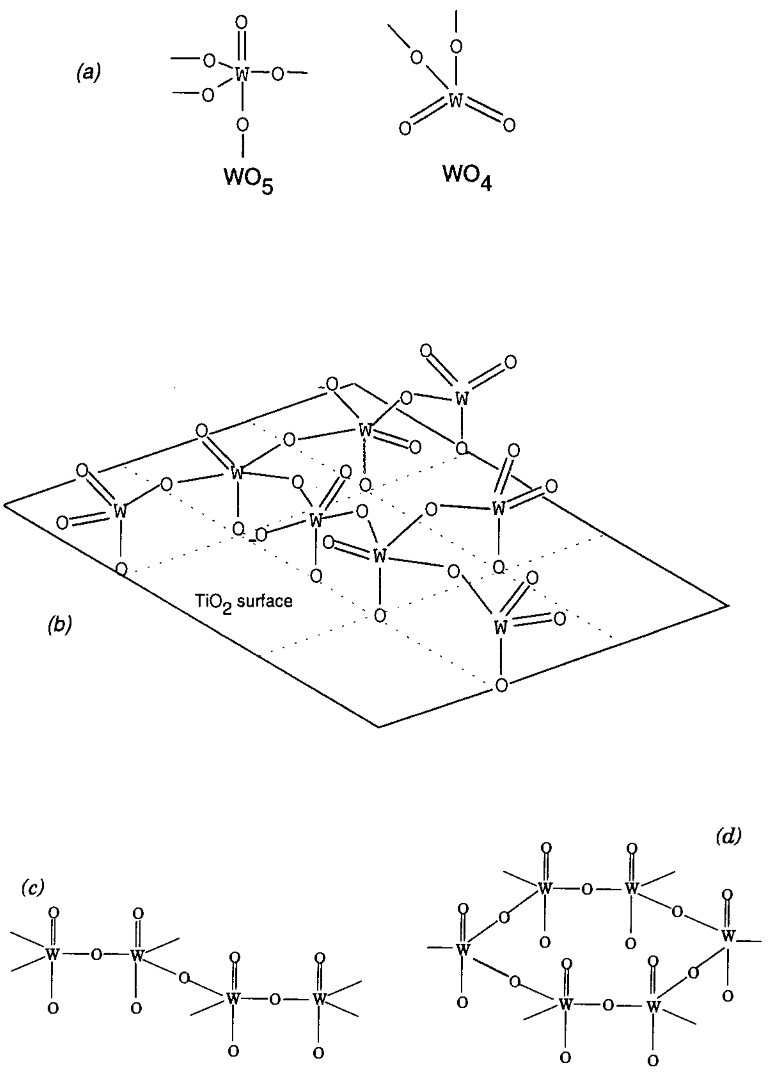

Fig. 2. (a) The structural polyhedra derived from XANES and EXAFS data by Hilbrig et al. [5]. (b) Schematic representation of the Hilbrig et al. model for the overlayer structure. (c) An alternative way to connect WO_5 units that gives rise to a zig-zag chain. (d) A ring structure that, in principle, is possible by connecting WO_5 units as in (c).

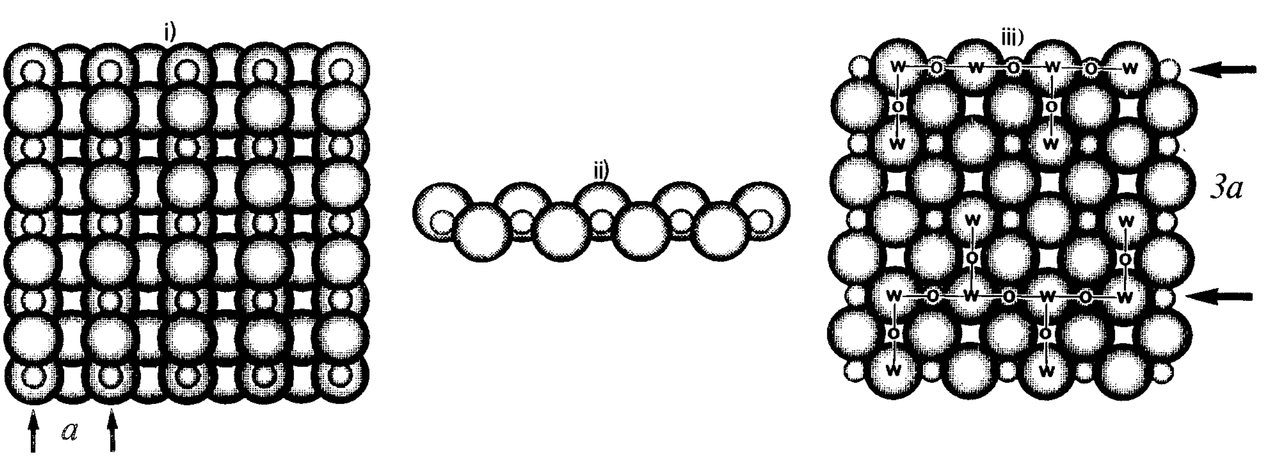

Fig. 3. (i) A view of the (001) surface from the plane normal, (ii) the corresponding side view and (iii) parallel straight chains of WO_5 that bridge a distance equivalent to 3.785 Å (these chains can be terminated either side of the chain spine).

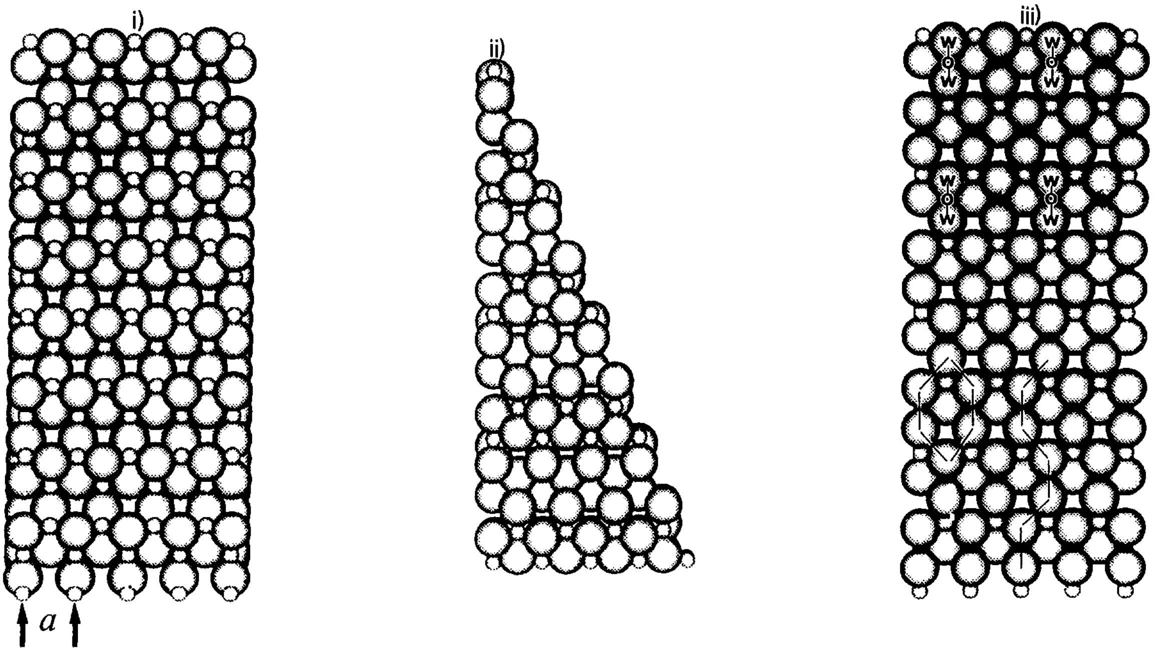

Fig. 4. (i) A view of the (011) surface from the plane normal, (ii) the corresponding side view and (iii) dimers of WO_4 units shown bridging a distance of 3 Å (the dotted lines indicate "intuitive" models that have been rejected).

various anatase surfaces requires some readjustment of the bond angles involved when these units are linked. Fig. 7a shows the ideal arrangement of two WO_5 units linked together with a W–O–W angle of 120°. In order to maintain the 1.91 Å W–O distance derived from the EXAFS data, the W–W distance is necessarily 3.31 Å. Therefore, O–O periodicities on the exposed substrate plane shorter than this require the W–O–W angle to be reduced resulting in compression of the W–O–W linkage. This is shown schematically in fig. 7b. Conversely, a periodicity greater than 3.31 Å means the W–O–W link would need to be "flattened" by increasing the W–O–W angle (shown in fig. 7c). The zig-zag chain arrangement proposed earlier for the WO_5 groups seems unlikely to

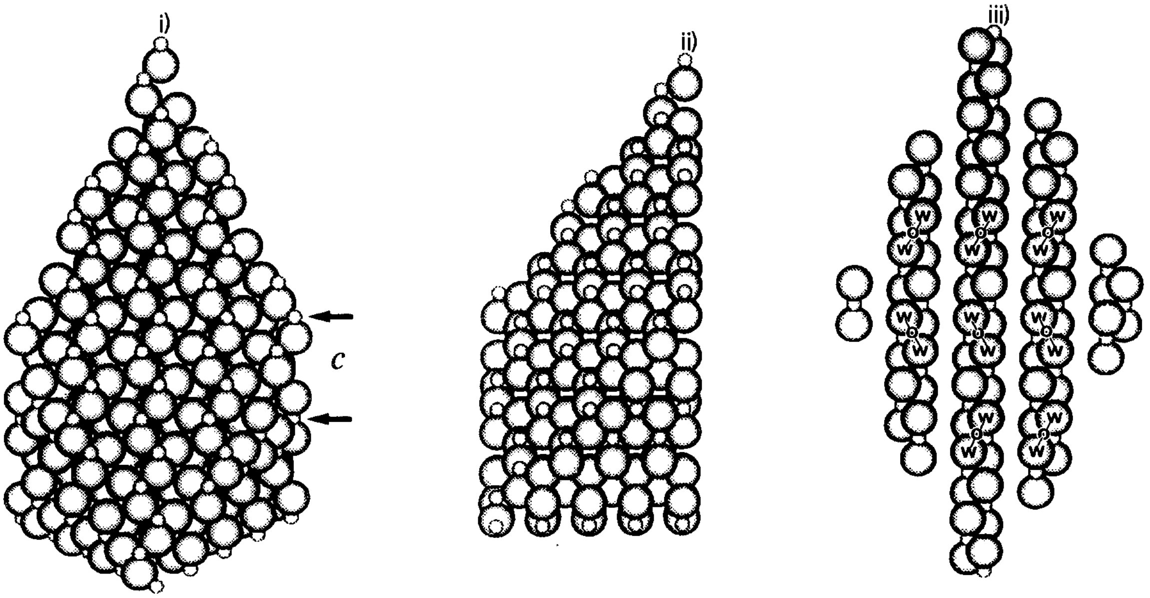

Fig. 5. (i) A view of the (112) surface from the plane normal, (ii) the corresponding side view and (iii) dimeric WO_4 units arranged on the anatase surface oxygen atoms for maximum density (the linking W–O–W bond spans a distance of 3.13 Å).

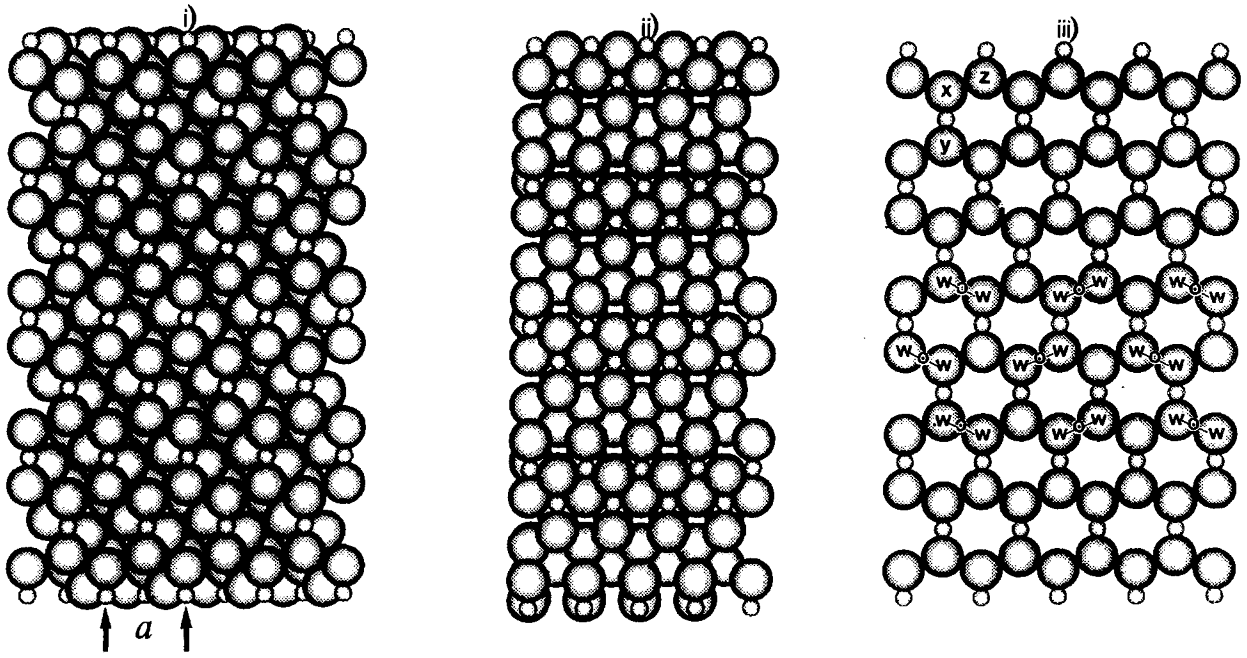

Fig. 6. (i) A view of the (110) surface from the plane normal, (ii) the corresponding side view and (iii) dimeric WO_4 units shown bridging a distance of 2.92 Å.

be able to accommodate similar structural distortions not least because the W–O bond length would have to change.

For the termination connections of WO_5 chains, the situation becomes more complex since the theoretical W–O–W angles for an ideal tetrahedron would be 109.5°. Thus, if the tungsten atoms in the WO_5 and WO_4 groups are to be planar (with the plane of the W–O–W link perpendicular to the substrate), the appropriate bond angles have to be adjusted, for example, as shown in fig. 7d. This is the simplest arrangement that can be imagined to satisfy the condition of planar tungsten atoms whilst maintaining the 1.91 Å W–O bond length derived from EXAFS. In this case both W–O

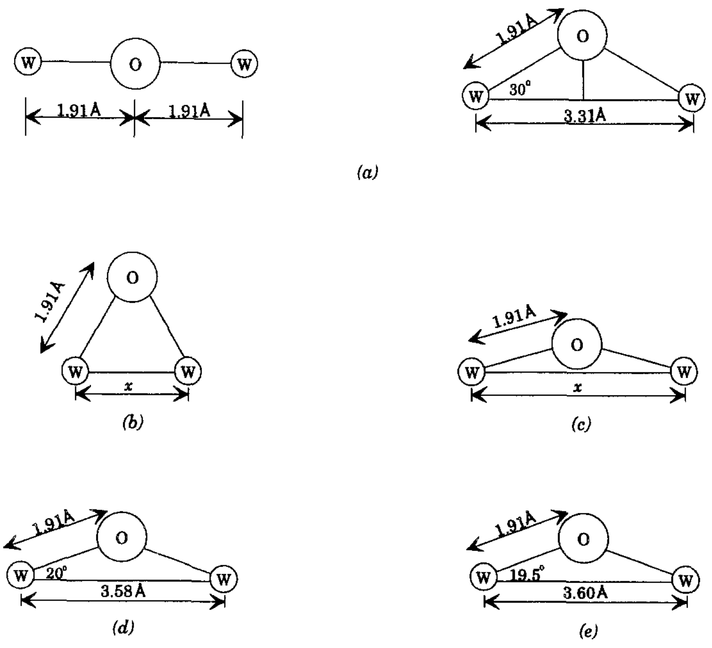

Fig. 7. (a) The idealised W–W distance envisaged between linked WO_5 units with model trigonal bipyramid symmetry. The effect on the W–W distance (x) and W–O–W angle when anchoring chains to an O–O distance that is (b) shorter than the ideal and (c) longer than the ideal. (d) The idealised W–W distance for a chain terminating bond. (e) Two ideal tetrahedral units combined to form a WO_4 dimer.

bonds in the two groups are inclined to the substrate plane by 20° with a W–O–W angle of 140° and a distance between tungsten atoms of 3.58 Å. In the discussion of the models that follows, this "ideal" termination distance will be referred to when considering the O–O distance that a terminating connection has to bridge across. Therefore, similar arguments to the case for adjusting the W–O–W angle in WO_5 links will be applied, i.e. if the O–O distance is shorter than 3.58 Å, it is accounted for by a corresponding decrease in the W–O–W angle and vice versa. It is acknowledged the situation is far more complicated than this since altering the inclination of the W–O bond in the WO_5 unit would almost certainly have implications for the rest of the chain, irrespective of how it is linked together. Furthermore, there is another feasible way of connecting idealised tetrahedral and trigonal bipyramidal groups *without* altering the respective angles. In this case, the bridging oxygen can be twisted out of the W–O–W plane which has been assumed to remain normal to the substrate plane.

Straight (i.e. not branched) chains appear to be possible on the (001) surface, as shown in fig. 3. The WO_5 units would span, in effect, the distance corresponding to the *a* or *b* lattice parameter of anatase (3.785 Å) which is roughly equivalent to tungsten atoms interconnected via 1.91 Å W–O bonds. Thus, the W–O–W bond angle has to increase to approximately 165° resulting in the idealised W–W distance extending from 3.31 Å by 13% (an example of the bond adjustment shown in fig. 7b). In this arrangement, underlying Ti^{4+} ions in the support can stabilise bridging oxygens between WO_5 groups. To preserve the 6+ oxidation state of tungsten, this structure precludes the possibility of branched chains and therefore parallel chains of WO_5 units are considered the most likely arrangement. These can be terminated by WO_4 units either side of the spine on this surface, probably alternately to avoid any steric hindrance between the double bonded oxygens of the WO_5 groups. For the same reason, parallel chains are shown to be separated by a distance corresponding to 3*a*, i.e. 11.355 Å. To anchor a WO_4 terminating group to the surface, the W–W distance has to increase from the idealised termination value of 3.58 to 3.785 Å (~ 5%). Neither zig-zag chains nor closed ring structures are reasonable propositions for this surface due to the absence of oxygen atoms in suitable positions for the appropriate W–O–Ti anchoring bonds.

The (011) surface shown in fig. 4 also appears at first sight to be capable of accommodating straight chains with the WO_5 groups separated by the *a* or *b* lattice parameter of anatase (with a corresponding increase in the W–O–W bond angle to roughly 165°). However, the terminating connection on this surface could only occur on one side of the chain backbone. This is due to the absence of planar oxygen atoms within a realistic distance on one side of the spine to allow the tetrahedrally coordinated tungsten atom to form the necessary W–O–Ti anchoring bond (the nearest is 9 Å). With the terminating connections all on one side there is then the problem of steric hindrance between double bonded oxygens on the WO_4 terminating groups. After considering many possibilities, it is more likely that the overlayer would consist of dimeric WO_4 units arranged on the surface in the manner shown on fig. 4iii. If model tetrahedra are assumed, then the ideal W–W distance would correspond to 3.6 Å as shown in fig. 7e with a W–O–W angle of 142°. Again, to fit this arrangement to different O–O distances whilst maintaining a 1.91 Å W–O bond length, the W–O–W angle is adjusted as described earlier. Thus, since the appropriate O–O distance on the (011) surface is equivalent to 3 Å, the idealised dimer W–W distance is required to shorten by approximately 17% giving rise to a W–O–W angle of 104°. A zig-zag chain and a closed ring structure also seem possible at first glance for the (011) surface as indicated by dashed lines. Both have been ruled out on the grounds that the resulting 3 Å W–O–W distance between WO_5 units is too short to allow a linear interconnecting oxygen atom without buckling the whole structure (or else changing the bond lengths).

The (112) surface (fig. 5) shows alternating rows of oxygen atoms that intuitively appear to be capable of accommodating a zig-zag chain. However, two reasons prevent this particular model from being realistic, namely (i) the distance between the oxygen atoms is too short at 3.13 Å and (ii) for a W–O–W bridge to occur, the branching W–O–W bonds would need to span a distance of approximately 6 Å. Thus, dimers of WO_4 groups are proposed, where the W–O–W link bridges the 3.13 Å distance between planar anatase oxygen atoms. In this case, the idealised dimer distance has to shorten by roughly 13% resulting in a W–O–W angle of approximately 110°. The inter dimer separation has been chosen to minimise steric hindrance effects.

Dimers of WO_4 groups also appear the most likely structure for the overlayer on the (110) plane (fig. 6) even though at first glance closed rings or zig-zag chains seem possible. However, neither of these models are really practical since for this projection (though not immediately obvious from fig. 6), only those surface oxygens of the type marked "x" and "y" are actually planar. The O–O distance between one of these positions and an oxygen atom at "z" (the next connecting oxygen point) is in fact a projected distance of 2.92 Å. Hence, in the case of a zig-zag chain, which necessarily has linear bridging W–O–W bonds, this would mean the structural units would have to follow a corrugated surface which seems unlikely. A similar argument applies to a ring structure but additionally there is an O–O distance of 3.9 Å for WO_5 units to bridge across, corresponding to the vertical sides of a rough hexagon. Consideration of the resulting geometry indicates that unless the W–O bond length can deviate from 1.91 Å this arrangement could not be satisfied. Hence, in fig. 6iii, dimers of WO_4 are shown bridging the projected distance of 2.92 Å.

This suggestion of dimeric WO_4 species for the overlayer (which can also be applied to the (001) surface) is not inconceivable since Horsley et al. [4] postulated similar structures for WO_3 on alumina catalysts containing 1/3 of a monolayer or less of tungsten oxide. Furthermore, since the W=O bond is likely to be the active centre of the initial reaction step in the SCR of NO_x gases, it is interesting to note that WO_4 dimers provide the greatest density of such bonds when anchored to the (112) and (110) surfaces (and experimentally, {112} surfaces are the most common anatase surfaces exposed).

3.2. Experimental observations of the tungsten oxide overlayer

Fig. 1c illustrated that contrast from the tungsten oxide overlayer gives rise to clusters with a projected pseudo-hexagonal shape. It also shows that these clusters exhibit a fringe structure roughly aligned in the same sense with respect to the substrate, implying definite epitaxial relationships exist between the tungsten oxide clusters and the different planes of the TiO_2 support. The lateral extent of the clusters has been found to be around 6–30 Å which is comparable to a typical facet dimension on the support and they cover up to approximately 50% of the projected surface area of the anatase grains. Fig. 1c also shows that as a result of viewing an approximately spherical grain in projection, there is an apparent increase in cluster density towards the titania particle edges. Measurements of equivalent fringe periodicities within typical clusters have revealed that they vary non-systematically with position on the grain. For instance, measurements from a high magnification micrograph of a typical support grain, fig. 8, show that the fringe periodicity ranges from 1.97 to 2.75 Å. If the assumption is made that the contrast originating from the clusters is almost entirely due to tungsten scattering centres, it is found that the measured spacings bear little resemblance to those expected for structures consisting of branched chains or indeed closed rings. It is also difficult to imagine a particular orientation that would give rise to projected pseudo hexagonal symmetry for lines of dimeric WO_4 units. Furthermore, fig. 9 shows a frame captured from a video recording using the low light level TV camera. Hexagonal-shaped clusters are just about visible

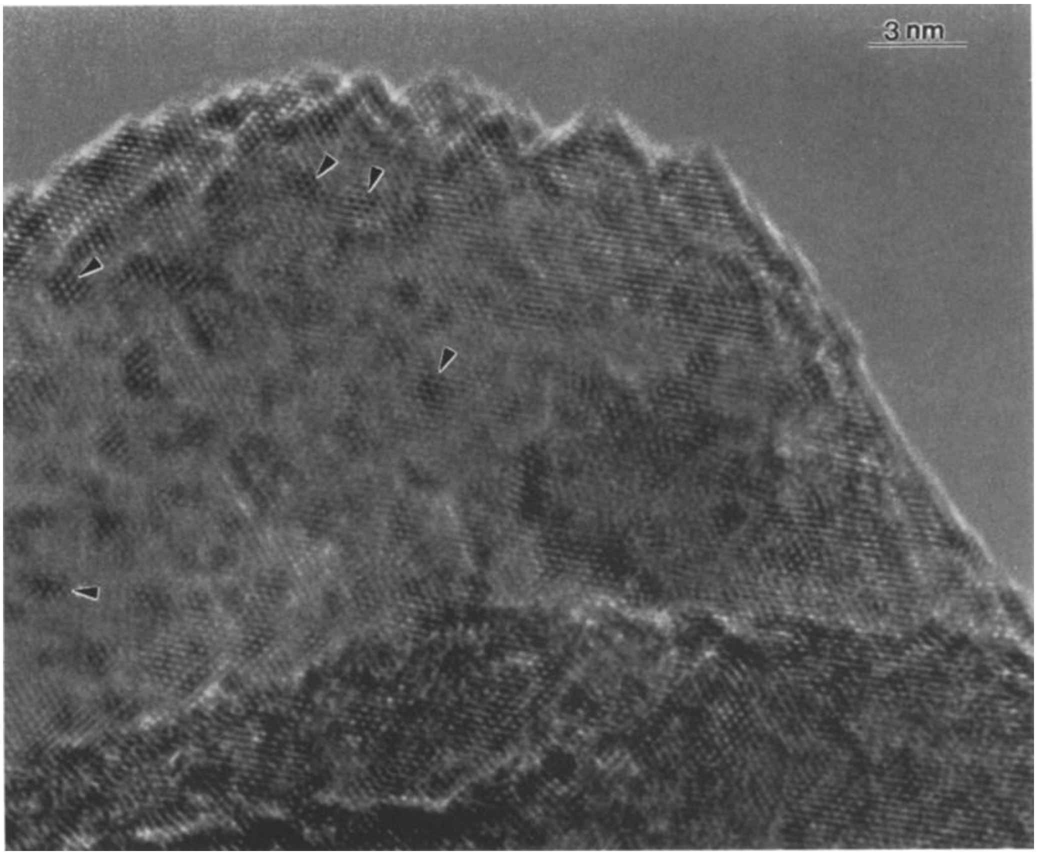

Fig. 8. Pseudo-hexagonal tungsten oxide clusters (arrowed) on the support in the WO_3/TiO_2 catalyst.

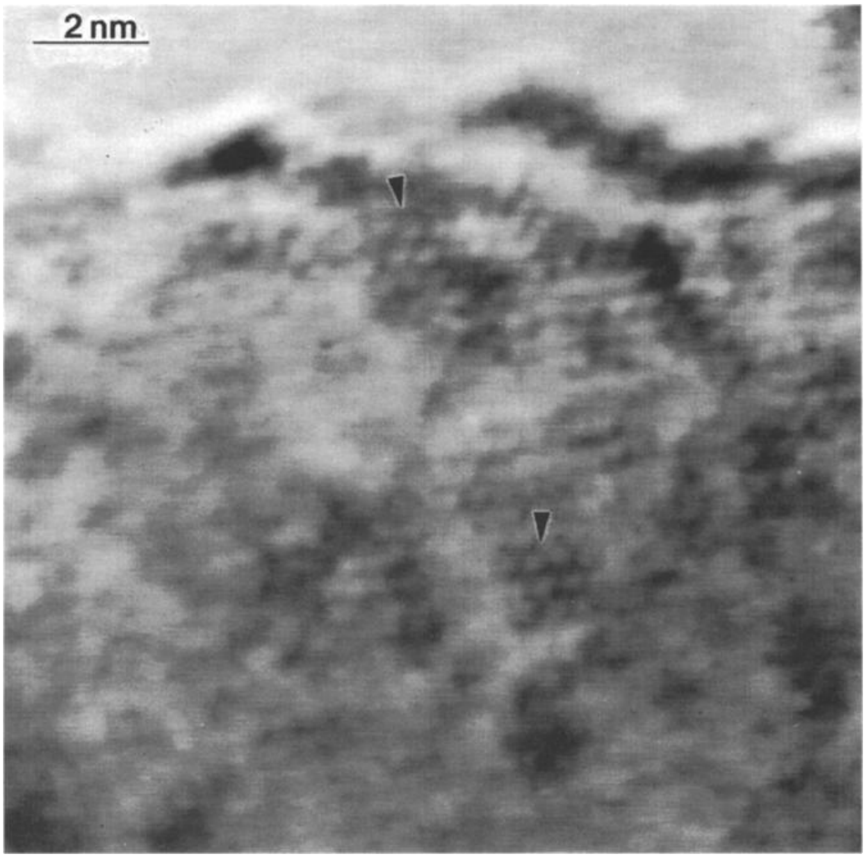

Fig. 9. An individual frame captured from a video recording showing that hexagonal shaped clusters (arrowed) are present even under low electron dose conditions.

(arrowed on the figure) with spacings comparable to those measured in fig. 8. There are at least three possibilities to explain the discrepancy between experimental observations and the theoretical models proposed earlier.

(i) The structural models for the overlayer are not correct.

(ii) The models are correct but the discrepancy is caused by reconstruction of the underlying titania surfaces.

(iii) The observations are compromised by electron beam damage.

The possibility that reduction of the overlayer takes place under the electron beam has been investigated by heavily irradiating anatase grains for several minutes. Such a grain is shown in fig. 10 on which there are now clusters exhibiting square arrays of "lattice" fringes, typically with a measured fringe periodicity of 2.2 ± 0.1 Å. Similar structures and spacings were observed by Tanaka et al. [11] after heavily irradiating thin amorphous films of tungsten oxide deposited on MgO to induce desorption of oxygen. It therefore seems conceivable that in fig. 10 reduction of the overlayer has gone to completion and the square-type of cluster corresponds to at least half a unit cell of metallic tungsten with a bcc structure viewed in projection along the [100] direction. Image simulations for the [100] zone axis of W are shown in fig. 11 for a thickness equivalent to one unit cell of tungsten at various microscope defoci to illustrate the square projection (the cross-fringes correspond to 2.233 Å {011} type planes of tungsten).

Thus we have considered that the "hexagonal-shaped" features observed derive from a partially reduced, non-stoichiometric tungsten oxide such as $W_{18}O_{49}$ [12] or $W_{24}O_{68}$ [13] or from islands of WO_2. WO_2 has a monoclinic distorted rutile structure [14] and belongs to space group $P2_1/c$. An [010] projection of WO_2 would give rise to near hexagonal symmetry as the projected structure, fig. 12a, shows. Computer simulations of this projection are shown in fig. 12b for a variety of sample thicknesses and microscope defoci. The approximate hexagonal symmetry displayed is obvious, although it is difficult to give a precise figure for the thickness of a typical cluster. What seems likely, however, is that the thickness is below 10 Å since we have never observed them in profile. Although the observed fringes may result from WO_2, there are slight discrepancies in both the fringe periodicities and angles. These may be significant but could also be caused by the very thin nature of the overlayer or by the strain required to

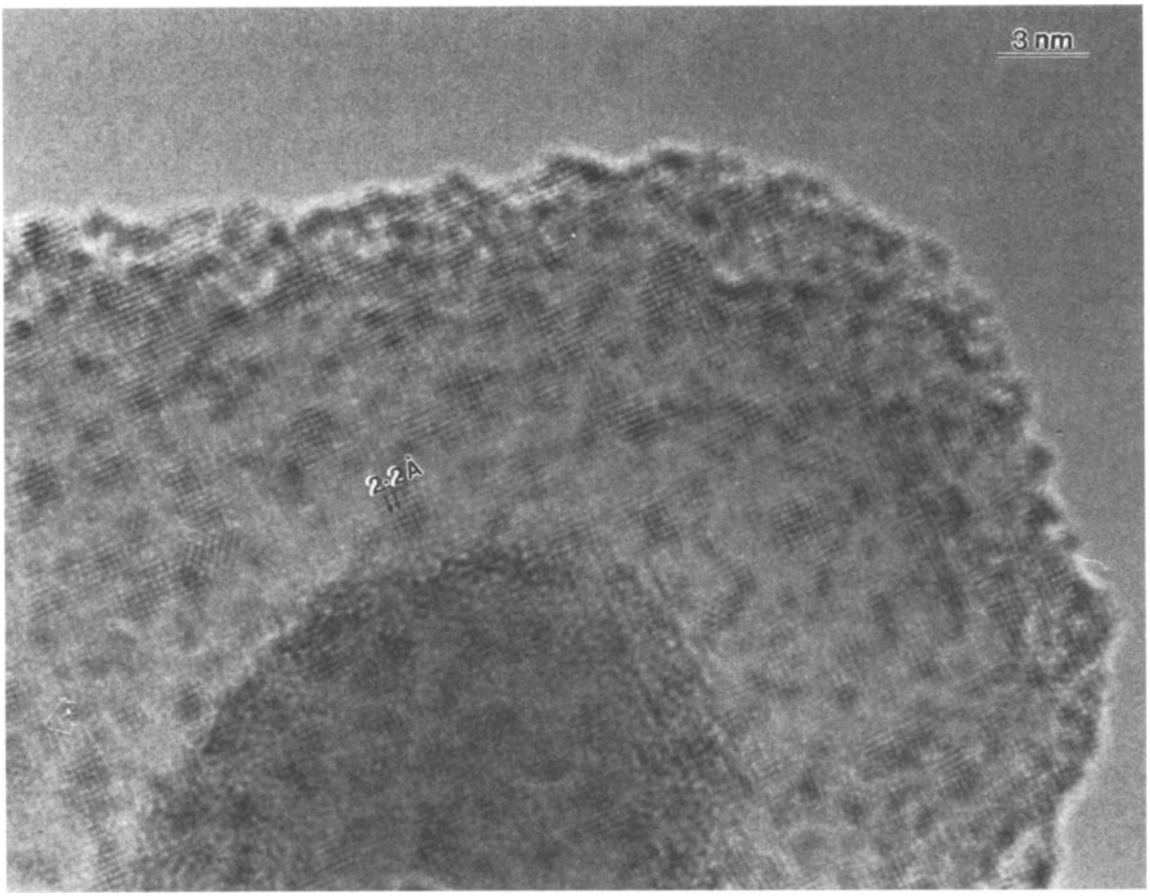

Fig. 10. Image of an anatase grain heavily irradiated by the electron beam giving rise to clusters exhibiting square arrays of "lattice" fringes with a 2.2 Å periodicity.

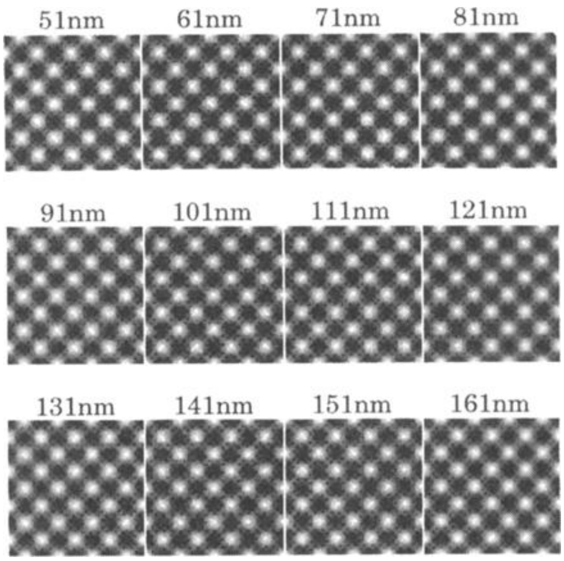

Fig. 11. Image simulations for a single unit cell of tungsten oriented on the [100] zone axis at different values of microscope defocus.

give a pseudo-morphic fit onto the substrate. We are therefore unable to go any further in determining why the structural model, which has a sound basis in EXAFS, XANES and other evidence (and has many attractive features) does not appear to be compatible with the electron microscopy observations.

4. Conclusions

After comparing two pure standard samples of anatase TiO_2 (one uncalcined, the other calcined in wet air) with a WO_3/TiO_2 catalyst, it is apparent the tungsten oxide overlayer preserves the surface roughness of the anatase observed in the uncalcined material. The grains of the support have also been found to adopt particular crystallographic habits and frequently expose {112}, {011}, {110} and {001} type facet planes. Overall, though, this study has demonstrated that HREM *may be* too disruptive a technique to characterise the structure of the tungsten oxide overlayer. However, when surface facet plane information about the TiO_2 support derived from TEM observations is combined with bond length and structural group data obtained from techniques

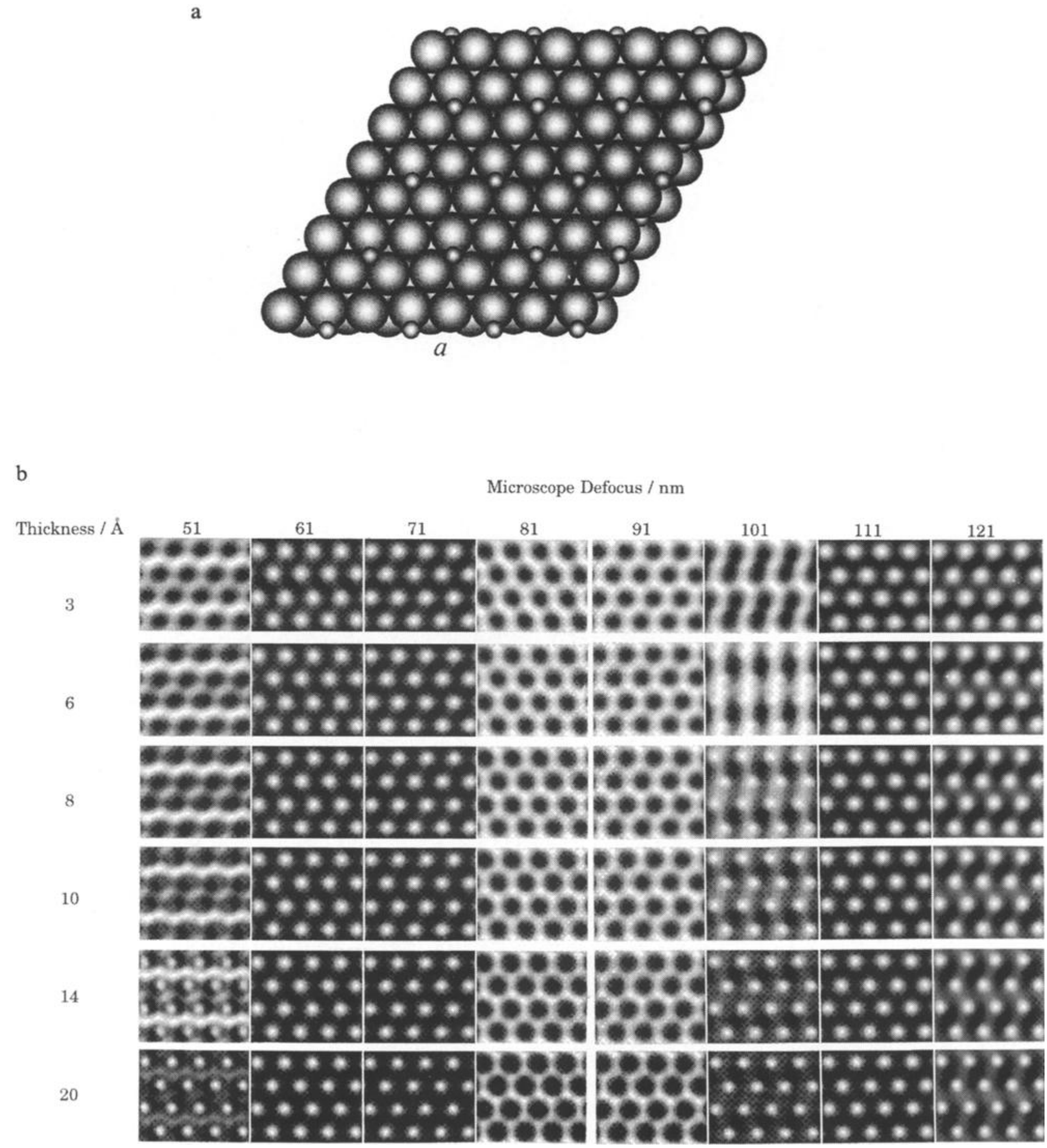

Fig. 12. (a) The [010] projected structure of WO_2. (b) Image simulations of the WO_2 [010] zone axis at various values of thickness and microscope defocus.

such as EXAFS and XANES, plausible structural models for the overlayer can be proposed. Indeed, we believe this methodology can be applied to other so-called monolayer catalytic systems. Thus, theoretical analysis of the WO_3/TiO_2 system suggests that the {112}, {011} and {110} anatase surfaces seem best suited to accommodating WO_4 dimers whereas the (001) surface appears capable of supporting both chainlike structures *and* WO_4 dimers. We acknowledge that the basis for our modelling may be oversimplified and a more critical examination of the proposed structures through the use of ab initio calculations is necessary.

Acknowledgement

We would like to thank EPSRC for their financial support during the course of this work and Professor R.C. Pond for useful discussions about the structure of WO_3.

References

[1] K.C. Taylor, in: *Catalysis – Science and Technology*, Vol. 5, eds. J.R. Anderson and M. Boudart (Springer, Berlin, 1984) p. 119.
[2] H. Bosch and F. Janssen, Catal. Today 2 (1988) 369.
[3] G.C. Bond and J.C. Védrine, Catal. Today 20 (1994) Parts 1–6.
[4] J.A. Horsley, I.E. Wachs, J.M. Brown, G.H. Via and F.D. Hardcastle, J. Phys. Chem. 91 (1987) 4014.
[5] F. Hilbrig, H.E. Göbel, H. Knözinger, H. Schmelz and B. Lengeler, J. Phys. Chem. 95 (1991) 6973.
[6] F. Hilbrig, H. Schmelz and H. Knözinger, *Proc. 10th Int. Conf. on Catalysis*, Budapest 1992 (Elsevier, Amsterdam, 1993) p. 1351.
[7] S.D. Berger, J.M. Macaulay and L.M. Brown, Phil. Mag. Lett. 56 (5) (1987) 179.
[8] S.R. Singh and L.D. Marks, Phil. Mag. Lett. 60 (1) (1989) 31.
[9] P.A. Stadelmann, Ultramicroscopy 21 (1987) 131.
[10] G.C. Bond, S. Flamerz and L.V. Wijk, Catal. Today 1 (1987) 229.
[11] N. Tanaka, T. Kitagawa and T. Kuzuka, Mater. Sci. Eng. B 19 (1993) 53.
[12] A. Magnéli, Ark. Kemi 1 (1949) 223.
[13] M. Sundberg, Chem. Scripta 14 (1978) 161.
[14] D.J. Palmer and P.G. Dickens, Acta Cryst. B 35 (1979) 2199.